Thermochimica Acta, 239 (1994) 73–85
Elsevier Science B.V., Amsterdam
SSDI 0040-6031(93)01623-B

Thermal investigation and stereochemical studies of some cyclic ligand complexes of nickel(II), copper(II), zinc(II) and cadmium(II) in the solid state.
Part 2

Samiran Mitra [a,*], Parimal Kundu [a] and Rajkumar Bhubon Singh [b]

[a] *Department of Chemistry, Inorganic Section, Jadavpur University, Calcutta-700 032, India*

[b] *Department of Chemistry, Manipur University, Canchipur, Imphal-795 003, India*

(Received 8 September 1993; accepted 30 September 1993)

Abstract

N-methylmorpholine (Mmorph) and *N,N'*-dimethylpiperazine (DMP) complexes of nickel(II), copper(II), zinc(II) and cadmium(II) were synthesized. Thermal investigations were carried out and the stereochemical changes that occur during the thermal decomposition reactions were studied. The complexes were found to have the following compositions $[Ni(Mmorph)Br_2] \cdot H_2O$, $[Cu(Mmorph)Br_2] \cdot H_2O$, $[Zn(Mmorph)_2Br_2]$, $[Ni(DMP)_2(H_2O)_2Br_2]$, $[Cu(DMP)Br_2]$, $[2ZnBr_2 \cdot 3DMP]$, and $[Cd(DMP)Br_2]$. Attempts to prepare a methylmorpholine complex of $CdBr_2$ failed. Some intermediate complexes were isolated using a temperature-arrest technique (pyrolysis). The characterization and study of the conformational and configurational changes were carried out using elemental and thermal analyses, IR spectral data and magnetic moment measurements. Most of the complexes of methylmorpholine and dimethylpiperazine appeared to be tetrahedral; however, $[Zn(Mmorph)_2Br_2]$, $[Ni(DMP)_2(H_2O)_2Br_2]$ and $[2ZnBr_2 \cdot 3DMP]$ are octahedral. The thermodynamic parameters such as activation energy E_a^*, enthalpy change ΔH, and entropy change ΔS were evaluated for the dehydration steps and decomposition reactions of the complexes using some standard methods and their values compared. The stability trend of the complexes with respect to activation energy is compared. A linear correlation obtained by plotting E_a^* against ΔS values showed that a system with a higher entropy change ΔS will require less energy E_a^* for its thermal decomposition.

INTRODUCTION

Although there are reports on acyclic ligand complexes in the literature, information on cyclic ligand complexes is relatively scarce [1–4]. We have attempted to synthesize some cyclic ligand (six-membered ring) complexes of transition and non-transition metal ions and have studied their stereochemical changes during thermal decomposition. In continuation of our

---

[*] Corresponding author.

earlier research [5, 6], the present work involves the thermal investigation and stereochemical studies of the complexes of Ni(II), Cu(II), Zn(II) and Cd(II) with methylmorpholine (Mmorph) and dimethylpiperazine (DMP) as cyclic ligands.

On pyrolysis, these complexes first undergo dehydration followed by decomposition in single or multiple steps. It is observed that before heating, the cyclic ligand functions as a chelate in most of the complexes. This is shown by the appearance of additional infrared-active bands in the range 700–1400 cm^{-1}, as compared to the free ligand [5, 7, 8]. In some cases the cyclic ligand functions as a bridging bidentate chelate [4, 7, 9, 10] and the bromide ions function as bridging bidentate or terminal unidentate chelates [5]. If these complexes are heated under non-isothermal conditions, they decompose via some intermediates (stable or unstable) in which the cyclic ligand functions as a bidentate chelate.

This kind of conformational change of the ligand is confirmed by the IR spectral data. Some thermodynamic parameters such as activation energy E_a^*, enthalpy change ΔH, and entropy change ΔS for the dehydration and decomposition reactions of the complexes in the solid state were computed with some standard equations and compared. Some useful conclusions relating to the thermal stability of the complexes are drawn.

EXPERIMENTAL

Materials and methods

The metal bromides were freshly prepared by neutralizing concentrated hydrobromic acid (AnalaR grade) solution with the corresponding metal carbonate (AnalaR grade), and subsequently crystallizing the required bromide from the filtrate obtained.

N-methylmorpholine (Fluka, Switzerland) and *N,N'*-dimethylpiperazine (Aldrich, USA) were used as-received. Ethanol and diethylether were dried using standard procedures [11].

Preparation of the complexes

For the preparation of $[Ni(Mmorph)Br_2] \cdot H_2O$ (1a), a clear solution of freshly prepared nickel bromide (0.500 g, 2 mmol) in dry ethanol (50 cm^3) was treated with the ligand (approx. 0.5 g, 5 mmol) in dry ethanol (30 cm^3) with constant stirring. A green nickel(II) complex was obtained. The complex was collected by filtration under suction, washed with dry ethanol (5 times), and then with a little dry diethylether (3 times), and was kept over fused calcium chloride in a desiccator: yield, 0.745 g, approx. 70%.

Complexes $[Cu(Mmorph)Br_2] \cdot H_2O$, $[Zn(Mmorph)_2Br_2]$, $[Ni(DMP)_2(H_2O)_2Br_2]$, $[Cu(DMP)Br_2]$, $[2ZnBr_2 \cdot 3DMP]$ and $[Cd(DMP)Br_2]$ were synthesized similarly.

Nickel, copper, zinc and cadmium were estimated gravimetrically by standard procedures [12]. The carbon, hydrogen and nitrogen contents were determined using a Carlo Erba 1106 elemental analyser. The elemental analyses are given in the Table 1. Thermal investigations (DTA and TGA) were carried out using a Shimadzu DT-30 thermal analyser under nitrogen atmosphere with a heating rate of 10°C min^{-1} (1°C min^{-1} for intermediate complexes) and α-alumina as a standard. Indium metal was used as a calibrant for the evaluation of enthalpy changes. IR spectra were recorded using Perkin-Elmer 363, 597, 783 and 843 models in KBr/CsI discs.

The effective magnetic moments were evaluated at room temperature from the magnetic susceptibility measurements with an EG and G PAR 155 vibrating-sample magnetometer.

RESULTS AND DISCUSSION

$[Ni(Mmorph)Br_2]\cdot H_2O$ (1a), $[Cu(Mmorph)Br_2]\cdot H_2O$ (2a) and $[Cd(DMP)Br_2]$ (7a)

These complexes have not been reported in the literature. On heating, complexes (1a), (2a) and (7a) decompose into their metal bromides via the intermediates $[Ni(Mmorph)_{0.5}Br_2]$ (1b), $[Cu(Mmorph)_{0.5}Br_2]$ (2b) and $[Cu(DMP)_{0.5}Br_2]$ (7b), as indicated in the TGA curves (Figs. 1 and 2). The corresponding TG temperature ranges and DTA peak temperatures are given in Table 2. The activation energies E_a^* were evaluated from the TGA curves using the equations of Horowitz and Metzger [13], Coats and Redfern [14] and Freeman and Carroll [15], and from the DTA curves using the equation of Borchardt and Daniels [16] (Table 2). The ΔH values for the conversions (1a) → (1b) and (1b) → $NiBr_2$, (2a) → (2b) and (2b) → $CuBr_2$ and (7a) → (7b) and (7b) → $CuBr_2$, were found to be 56 and 25, 19 and 71, and 12 and 23 kJ mol^{-1}, respectively. The ΔS values were evaluated from the relation $\Delta S = \Delta H/T_m$, where T_m is the DTA peak temperature in kelvin [17], see Table 2.

In all the complexes (1a), (2a) and (7a), the cyclic ligands act as a bridge and exist in the chair form [5, 7, 8], as shown by the IR absorption bands (Table 3), and are expected to be tetrahedral and polymeric. The intermediate complexes could not be isolated. The values of the effective magnetic moment for complexes (1a) and (2a) are 2.91 and 2.02 BM respectively. The probable paths of the decomposition reactions are given in the Scheme 1.

$[Zn(Mmorph)_2Br_2]$ (3a) and $[Ni(DMP)_2(H_2O)_2Br_2]$ (4a)

Complexes (3a) and (4a) have not been reported earlier. The presence of coordinated water molecules in complex (4a) was confirmed by the appearance of IR bands [4, 5, 18] at 3400 and 3300 cm^{-1} for $\nu(OH)$, at 1650, 1640

TABLE 1

Analytical data (calculated values in parentheses) and effective magnetic moment values of cyclic ligand [a] complexes of Ni(II), Cu(II), Zn(II) and Cd(II)

No.	Complex	Colour	Analysis %				μ_{eff}/BM
			Metal	Carbon	Nitrogen	Hydrogen	
(1a)	$[\mathrm{NiL'Br_2}]\cdot\mathrm{H_2O}$	Green	16.80 (16.88)	17.25 (17.25)	3.70 (3.73)	4.00 (4.02)	2.91
(2a)	$[\mathrm{CuL'Br_2}]\cdot\mathrm{H_2O}$	Deep green	18.40 (18.55)	17.40 (17.51)	4.08 (4.07)	3.70 (3.79)	2.02
(3a)	$[\mathrm{ZnL'_2Br_2}]$	White	15.29 (15.09)	28.00 (28.07)	6.50 (6.55)	5.10 (5.15)	
(3b)	$[\mathrm{ZnL'Br_2}]$	White	20.00 (20.03)	18.30 (18.38)	4.20 (4.28)	3.20 (3.28)	
(4a)	$[\mathrm{NiL''_2(H_2O)_2Br_2}]$	Green	12.15 (12.15)	24.80 (24.86)	5.82 (5.80)	5.30 (5.38)	3.07
(4b)	$[\mathrm{NiL''Br_2}]$	Light chocolate	17.60 (17.64)	18.00 (18.03)	4.25 (4.20)	3.32 (3.30)	3.02
(5a)	$[\mathrm{CuL''Br_2}]$	Deep green	17.60 (17.75)	20.10 (20.13)	7.85 (7.83)	3.90 (3.91)	2.23
(6a)	$[\mathrm{2ZnBr_2\cdot 3DMP}]$	White	16.20 (16.39)	27.29 (27.24)	10.57 (10.59)	5.28 (5.29)	
(6b)	$[\mathrm{2ZnBr_2\cdot 2DMP}]$	White	19.10 (19.15)	21.14 (21.21)	8.22 (8.25)	2.69 (2.65)	
(7a)	$[\mathrm{CdL''Br_2}]$	White	28.70 (29.08)	18.50 (18.64)	7.24 (7.25)	3.50 (3.62)	

[a] L′ is *N*-methylmorpholine (Mmorph) and L″ is *N*,*N*′-dimethylpiperazine (DMP).

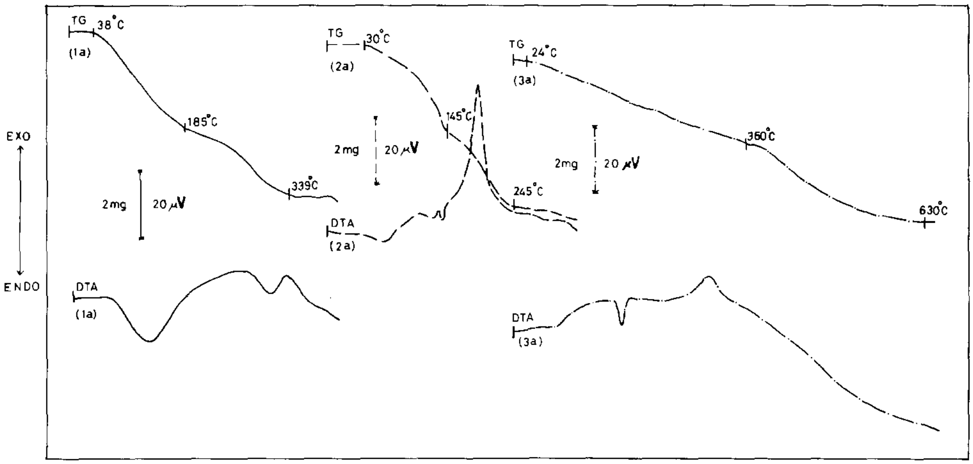

Fig. 1. Thermal curves of: ——, complex (1a), $[Ni(Morph)Br_2] \cdot H_2O$, sample mass 13.6 mg; – – –, complex (2a), $[Cu(Morph)Br_2] \cdot H_2O$, sample mass 13.8 mg; and – · – · –, complex (3a), $[Zn(Morph)_2Br_2]$, sample mass 10.6 mg.

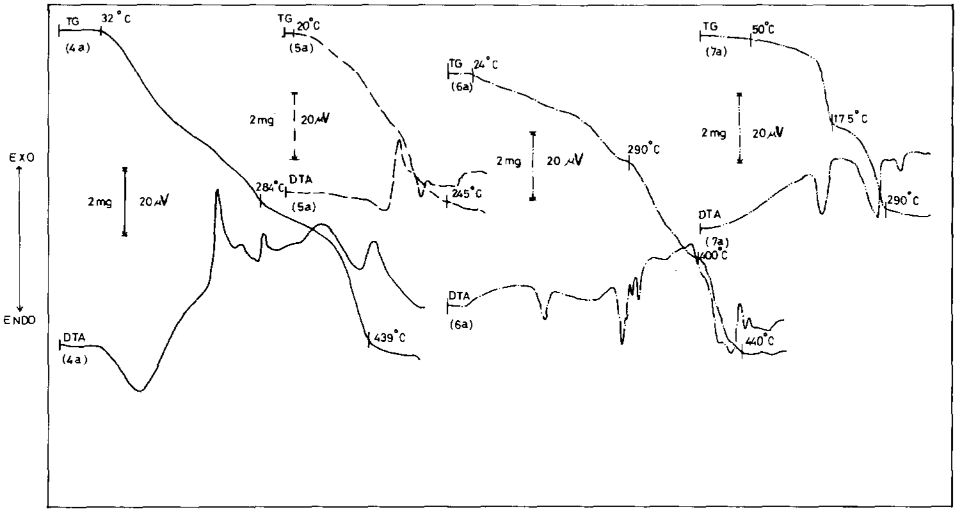

Fig. 2. Thermal curves of: ——, complex (4a), $[Ni(DMP)_2(H_2O)_2Br_2]$, sample mass 16.7 mg; – – –, complex (5a), $[Cu(DMP)Br_2]$, sample mass 14.8 mg; – · – · –, complex (6a), $[2ZnBr_2 \cdot 3DMP]$, sample mass 18.5 mg; and – · · – · · –, complex (7a), $[Cd(DMP)Br_2]$, sample mass 17.8 mg.

and 1620 cm^{-1} for δ(HOH), at 840, 820 and 790 cm^{-1} for ρ_r(HOH), at 566 cm^{-1} for ρ_w(HOH), and at 420 and 405 cm^{-1} for ν(Ni–OH_2). Furthermore, the weight losses in the TGA curves for complexes (3a) and (4a) in the ranges 24–350 and 32–284°C, together with the endothermic peaks at 140 and 73°C and the exothermic peaks at 210 and 282°C, respectively

TABLE 2

Thermal parameters of *N*-methylmorpholine (L′) and *N*,*N*′-dimethylpiperazine (L″) complexes of Ni(II), Cu(II), Zn(II) and Cd(II)

No.	Decomposition reactions		TG temp. range/°C	DTA peak temp./°C		E_a^*/(kJ mol^{-1}) [a] TG			DTA	Enthalpy change ΔH/(kJ mol^{-1})	Entropy change (ΔS)/(J K^{-1} mol^{-1})
				Exo.	Endo.	H.M.	C.R.	F.C.			
1(a)	$[\mathrm{NiL'Br_2}]\cdot\mathrm{H_2O}$	$\rightarrow[\mathrm{NiL'_{0.5}Br_2}]$	38–185	–	73	29	15	17	30	56	161
1(b)	$[\mathrm{NiL'_{0.5}Br_2}]$	$\rightarrow\mathrm{NiBr_2}$	186–339	315	293 [b]	75	39	60	106	25	44
2(a)	$[\mathrm{CuL'Br_2}]\cdot\mathrm{H_2O}$	$\rightarrow[\mathrm{CuL'_{0.5}Br_2}]$	30–145	–	56	40	21	18	33	19	56
2(b)	$[\mathrm{CuL'_{0.5}Br_2}]$	$\rightarrow\mathrm{CuBr_2}$	146–245	200	–	75	46	49	93	71	150
3(a)	$[\mathrm{ZnL'_2Br_2}]$	$\rightarrow[\mathrm{ZnL'Br_2}]$	24–350	–	140	15	12	10	8	12	29
3(b)	$[\mathrm{ZnL'Br_2}]$	$\rightarrow\mathrm{ZnBr_2}$	351–630	288	–	53	31	33	40	38	67
4(a)	$[\mathrm{NiL''_2(H_2O)_2Br_2}]$	$\rightarrow[\mathrm{NiL''Br_2}]$	32–284	210 282	73 [b]	20	8	10	67	42	121
4(b)	$[\mathrm{NiL''Br_2}]$	$\rightarrow\mathrm{NiBr_2}$	285–439	–	374	101	86	83	116	46	71
5(a)	$[\mathrm{uL''Br_2}]$	$\rightarrow\mathrm{CuBr_2}$	20–245	114 187	141 [b]	30	12	13	64	24	57
6(a)	$[\mathrm{2ZnBr_2\cdot 3L''}]$	$\rightarrow[\mathrm{2ZnBr_2\cdot 2L''}]$	24–290	280 [b]	142	19	8	24	54	14	25
6(b)	$[\mathrm{2ZnBr_2\cdot 2L''}]$	$\rightarrow[\mathrm{2ZnBr_2\cdot L''}]$	291–400	376 [b]	308	41	10	12	177	55	84
6(c)	$[\mathrm{2ZnB_2\cdot L''}]$	$\rightarrow\mathrm{2ZnBr_2}$	401–440	–	425	347	180	678	186	8	11
7(a)	$[\mathrm{CdL''Br_2}]$	$\rightarrow[\mathrm{CdL''_{0.5}Br_2}]$	50–175	–	155	59	41	35	130	12	28
7(b)	$[\mathrm{Cd''_{0.5}Br_2}]$	$\rightarrow\mathrm{CdBr_2}$	176–290	–	257	115	92	80	148	23	43

[a] H.M. means Horowitz and Metzger, C.R. means Coats and Redfern, F.C. means Freeman and Carroll. [b] DTA peak temperature used for the evaluation of ΔS.

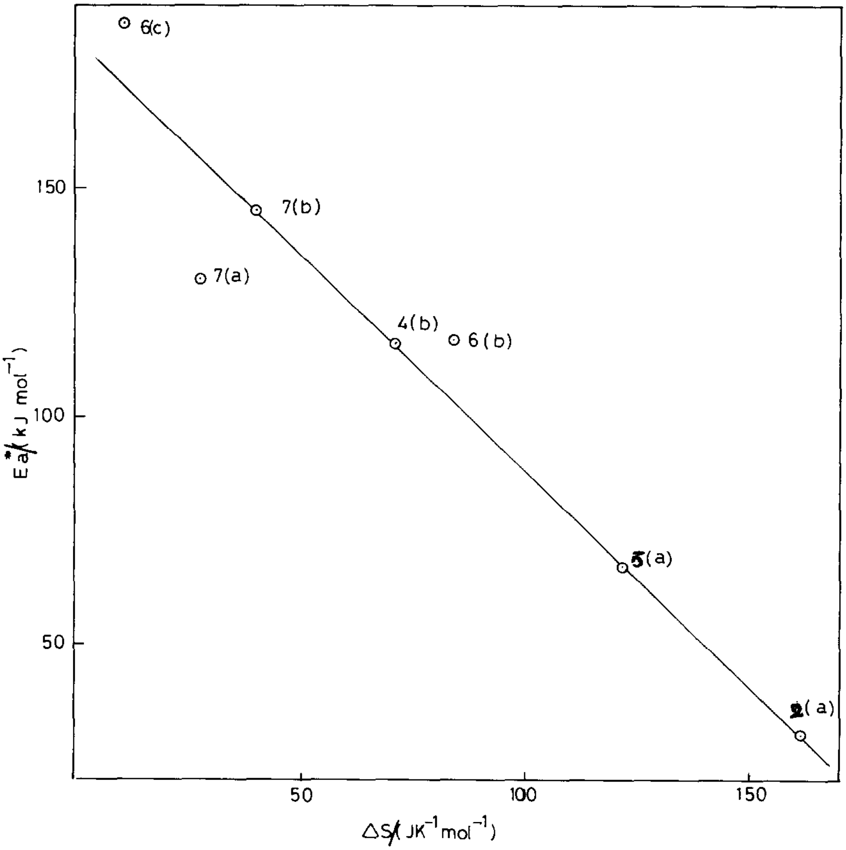

Fig. 3. Plots of E_a^* versus ΔS for the conversions: 2(a), $[Cu(Morph)Br_2] \longrightarrow [Cu(Morph)_{0.5}Br_2]$; 4(b), $[Ni(DMP)Br_2] \longrightarrow NiBr_2$; 5(a), $[Cu(DMP)Br_2] \longrightarrow CuBr_2$; 6(b), $[2ZnBr_2 \cdot DMP] \longrightarrow [2ZnBr_2 \cdot DMP]$; 6(c), $[2ZnBr_2 \cdot DMP] \longrightarrow 2ZnBr_2$; 7(a), $[Cd(DMP)Br_2] \longrightarrow [Cd(DMP)_{0.5}Br_2]$; and 7(b) $[Cd(DMP)_{0.5}Br_2] \longrightarrow CdBr_2$.

(Table 2), correspond to one molecule of cyclic ligand (with two molecules of water for complex (4a)). Complexes (3b) and (4b) were converted into the metal bromides in the ranges 351–630 and 285–439°C, with an exothermic peak at 288°C and an endothermic peak 374°C (Figs. 1 and 2). The IR absorption bands (Table 3) indicate that the cyclic ligand in the complex (3a) functions as a bidentate chelate (boat form) with respect to the free ligand (chair form) [7, 8] in the range 1400–700 cm^{-1}, and the bromide functions as a terminal unidentate ligand. In complex (4a), the cyclic ligand functions as a unidentate ligand and exists in the chair form. The effective magnetic moment ($\mu_{eff} = 3.07$ BM) also suggests that complex (4a) has an octahedral structure.

The intermediates (3b) and (4b) were isolated at around 345 and 280°C respectively, by keeping the heating rate at 1°C min^{-1} in the respective

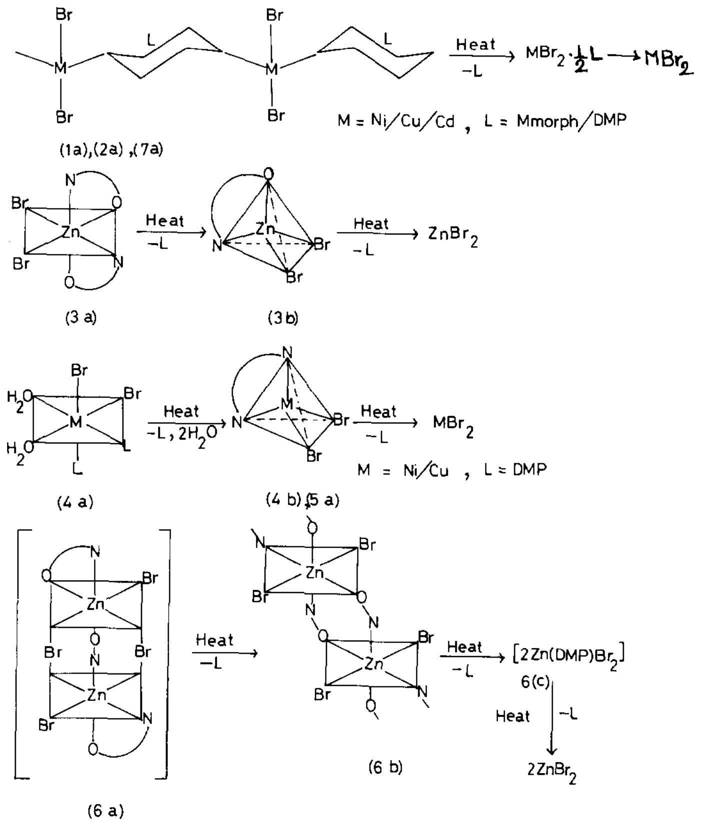

Scheme 1.

temperature ranges. In the complexes (3b) and (4b) the cyclic ligands exist in the boat form [4, 7], indicated by the IR spectral data (Table 3). The effective magnetic moment μ_{eff} of (4b) (3.02 BM) indicates that the complex is tetrahedral. The structures are shown in Scheme 1. Values of E_a^*, ΔH and ΔS are given in Table 2.

[Cu(DMP)Br_2] (5a)

Complex (5a) is monomeric and on heating, undergoes decomposition to $CuBr_2$ in a single step in the range 20–245°C, are reflected in the TGA curve. The corresponding exothermic DTA peaks are at 114 and 187°C and an endothermic peak appears at 141°C. In this complex, the cyclic ligand functions as a bidentate chelate (boat form) [4, 5, 7]. The value for the effective magnetic moment ($\mu_{\text{eff}} = 2.23$ BM) suggests that the complex may be in a tetrahedral configuration [5]. Values of E_a^*, ΔH and ΔS are given in Table 2. The decomposition path of complex (5a) is shown in the Scheme 1.

TABLE 3

IR spectral data[a] (cm^{-1}) for Ni(II), Cu(II), Zn(II) and Cd(II) cyclic ligand[b] complexes

$\nu(NH)$[c] + $\nu(OH)$	$\nu(CH_2)$	$\delta(NH)$[c] + $\delta(HOH)$	$\delta(CH_2)$	$\sigma(NH)$ + $\rho_W(NH)$ + $\sigma(CH_2)$	$\nu(CH)$ + $\nu(C-C)$ + $\nu_a(COC)$	$\rho_r(CH_2)$ + $\nu_S(COC)$ + $\rho_r(HOH)$	$\nu(M-L)$ + $\rho_W(HOH)$[c]	$\nu(M-Br)$
(1a) $[NiL'Br_2] \cdot H_2O$								
3427(s)	2864(s)	1691(s)	1494(s)	1384(s)	1186(w)	895(s)	467(s)	324(w)
3304(w)	2794(ms)	1666(ms)	1480(sh)	1335(ms)	1112(s)	845(w)	453(ms)	273(s)
3272(s)	2634(w)	1657(s)	1453(vs)	1308(w)	1109(w)	825(s)	429(ms)	241(w)
3234(vw)		1622(ms)		1273(s)	1048(sh)		390(s)	215(s)
3205(ms)		1613(sh)			1031(s)			
		1573(s)			988(ms)			
(2a) $[CuL'Br_2] \cdot H_2O$								
3418(vs)	2744(w)	1637(s)	1461(vs)	1358(ms)	1185(s)	849(s)	505(w)	389(ms)
3340(br)	2352(w)	1630(vs)	1394(s)	1310(s)	1122(ms)	811(ms)	451(s)	271(w)
3215(s)	2330(s)	1613(sh)		1273(vs)	1080(s)	784(ms)	422(w)	245(w)
		1516(w)		1261(w)	1041(w)		400(s)	
		1503(w)			988(s)			
(3a) $[ZnL'_2Br_2]$								
3461(ms)	2862(s)	1689(w)	1444(vs)	1386(ms)	1180(s)	893(s)	487(ms)	379(s)
3340(ms)	2795(w)	1581(w)	1412(s)	1361(s)	1148(ms)	876(ms)	482(s)	322(w)
3265(s)		1553(ms)	1400(sh)	1350(ms)	1137(ms)	820(ms)	396(w)	297(s)
3240(ms)		1516(s)		1303(s)	1080(vs)	767(s)		240(sh)
3160(w)		1502(s)		1278(s)	1070(ms)			225(s)
		1492(w)		1218(ms)	1063(ms)			205(w)
					1009(v)			

TABLE 3 (continued)

ν(NH)[c] + ν(OH)	$\nu(CH_2)$	δ(NH)[c] + δ(HOH)	$\delta(CH_2)$	σ(NH) + ρ_W(NH) + $\sigma(CH_2)$	ν(CH) + ν(C–C) + ν_a(COC)	$\rho_r(CH_2)$ + ν_S(COC) + ρ_r(HOH)	ν(M–L) + ρ_W(HOH)[c]	ν(M–Br)
(3b) [$ZnL'Br_2$]								
3475(s)	2765(s)	1620(s)	1445(ms)	1380(s)	1171(w)	830(s)	475(ms)	350(ms)
3345(ms)	2740(s)	1528(w)	1440(sh)	1295(ms)	1047(ms)	815(ms)	460(sh)	325(w)
3200(s)	2675(ms)	1487(s)	1415(ms)	1280(ms)	1020(w)	800(ms)	445(w)	300(w)
3195(br)				1260(sh)	1000(vw)	790(sh)	390(w)	215(s)
				1190(sh)	980(w)	772(s)		210(w)
(4a) [$NiL''_2(H_2O)_2Br_2)$]								
3400(sbr)	2912(w)	1690(w)	1470(ms)	1360(ms)	1105(s)	872(s)	566(s)	330(w)
3300(br)	2800(w)	1670(w)	1460(s)	1300(w)	1080(ms)	840(w)	480(s)	300(s)
3215(s)		1650(s)	1420(sh)	1280(ms)	1010(w)	820(w)	470(w)	280(ms)
3190(s)		1640(sh)		1195(w)	980(ms)	790(s)	420(sh)	265(s)
		1620(ms)				760(w)	405(ms)	
		1590(s)				720(ms)	395(s)	
(4b) [$NiL'Br_2$]								
3250(sbr)	2850(s)	1670(w)	1462(ms)	1380(ms)	1101(s)	885(s)	450(ms)	345(ms)
3200(s)	2782(ms)	1647(ms)	1450(s)	1362(sh)	1092(ms)	845(ms)	415(w)	340(sh)
3187(ms)	2690(sh)	1592(sh)	1410(w)	1292(s)	1085(sh)	830(sh)	400(w)	305(w)
3150(w)		1580(s)		1281(s)	1060(w)	730(w)		282(s)
		1520(ms)		1259(sh)	1045(w)	700(ms)		215(w)
					957(s)	635(s)		
						600(w)		

(5a) [CuL″Br_2]								
3321(br)	2820(w)	1672(s)	1465(s)	1374(vw)	1168(s)	888(s)	425(s)	300(w)
3200(w)	2682(s)	1666(sh)	1458(s)	1320(w)	1110(sh)	863(sh)	400(w)	290(w)
3120(vw)		1657(s)	1420(sh)	1285(br)	1051(s)	848(vs)	390(ms)	272(s)
		1650(sh)		1220(w)	1021(w)	810(s)		220(w)
				1200(sh)	981(sh)	711(vs)		
				1190(s)				
(6a) [2ZnBr_2 · 3L″]								
3293(vs)	2886(ms)	1689(w)	1484(vs)	1386(sh)	1180(s)	880(s)	487(s)	379(ms)
3235(br)	2836(ms)	1581(sh)	1142(ms)	1361(ms)	1137(s)	827(sh)	452(ms)	302(ms)
3115(ms)	2464(w)	1553(ms)	1413(sh)	1346(w)	1096(ms)	805(s)	396(ms)	240(w)
2985(s)		1516(ms)		1303(w)	1074(w)	790(w)		210(w)
				1278(ms)	1063(w)	762(s)		
				1218(w)	788(s)	735(ms)		
(6b) [2ZnBr_2 · 2L″]								
3400(sbr)	2857(s)	1680(w)	1432(w)	1380(w)	1142(s)	842(w)	480(w)	360(ms)
3392(sh)	2790(w)	1645(w)	1420(ms)	1370(vs)	1100(ms)	820(ms)	460(w)	350(sh)
3300(s)		1622(s)	1400(sh)	1320(w)	1087(sh)	800(sh)	450(ms)	282(w)
3215(s)				1300(ms)	997(w)	782(w)	415(sh)	222(s)
				1260(s)				
(7a) [CdL″Br_2]								
3240(br)	2880(w)	1660(w)	1475(sh)	1360(s)	1180(w)	820(vs)	460(vs)	345(w)
3100(s)	2850(s)	1640(w)	1460(s)	1300(s)	1160(s)	765(w)	420(ms)	305(s)
3000(sh)	2760(w)	2630(w)	1450(sh)	1280(ms)	1140(s)	630(ms)	400(vw)	280(w)
2980(w)			1390(w)	1200(w)	1110(ms)		395(s)	
					1100(ms)			
					980(vs)			

---

[a] Key: sbr, strong broad; ms, medium strong; br, broad; w, weak; vw, very weak; sh, shoulder; vs, very strong. [b] L′ is methylmorpholine (Mmorph); L″ is dimethylpiperazine (DMP). [c] Complexes containing H_2O molecules: bands for ν(NH), δ(NH) and ν(M-L) overlapped with bands ν(OH), δ(HOH) and ρ_W(HOH).

[$2ZnBr_2 \cdot 3DMP$] (6a)

This complex has not been reported before; it has a dimeric structure. On heating, complex (6a) decomposes to $ZnBr_2$ in three steps (losing one molecule of cyclic ligand for each step), as indicated in the TGA curve (Fig. 2). The TGA temperature ranges, DTA peak temperatures and values of E_a^*, ΔH and ΔS for the conversions (6a) → (6b), (6b) → (6c), and (6c) → $2ZnBr_2$ are given in Table 2. Before heating, the cyclic ligand functions as a bidentate chelate as well as a bridging bidentate ligand. Complex (6a) has an octahedral configuration about each zinc atom. This was confirmed by the infrared-active bands listed in Table 3.

The intermediate complex (6b) was isolated. The cyclic ligand functions as a bridging bidentate ligand and exists in the chair form [5, 6]. The complex is expected to be polymeric [7]. The possible steps of the decomposition reactions are given in Scheme 1.

It is also observed that the values of the activation energy calculated by the Horowitz and Metzger equation [13] are higher in most cases than the values evaluated by Coats and Redfern [14] and Freeman and Carroll [15] equations, as we have reported in other cases earlier [6].

The stability of the *N*-methylmorpholine complexes follows the trend Ni(II) < Cu(II) for the first and second step of the decomposition reactions. The stability order of the *N*,*N'*-dimethylpiperazine complexes follows the trend Ni(II) = Zn(II) < Cu(II), but the trend is reversed in the second step of the decomposition reaction (Table 2).

In addition, a linear correlation is obtained by plotting the values of E_a^* values ΔS (Fig. 3). It was found that a system having a higher entropy change will require less energy for its thermal decomposition.

ACKNOWLEDGEMENTS

The authors are grateful to the Regional Sophisticated Instrumentation Centres (C.D.R.I) at Lucknow, Madras and Shillong for the IR spectra and elemental analyses. Financial assistance from CSIR to P.K. is gratefully acknowledged.

REFERENCES

1 W.K. Musker and M.S. Hussain, Inorg. Chem., 8 (1969) 528.
2 J.M. Rigg and E. Sherwine, J. Inorg. Nucl. Chem., 27 (1965) 653.
3 M.N. Hughes and W.R. McWhinie, J. Inorg. Nucl. Chem., 28 (1966) 1659.
4 L.K. Singh and S. Mitra, J. Chem. Soc. Dalton Trans. A, (1987) 2089.
5 R.K.B. Singh and S. Mitra, Thermochim. Acta, 164 (1990) 365; 181 (1991) 289.
6 R.K.B. Singh and S. Mitra, Thermochim. Acta, 236 (1994) 175.
7 P.J. Hendra and D.B. Powell, J. Chem. Soc. A, (1960) 5105.
8 G.W.A. Fowles and R.A. Walton, J. Chem. Soc., (1964) 4330, 4953.
9 E.A. Allen, N.P. Johnson, D.T. Rosevear and W. Wilkinson, J. Chem. Soc. A, (1970) 2137.

10 I.S. Ahuja and R. Singh, J. Coord. Chem., 5 (1976) 167.
11 A.I. Vogel, A Text Book of Practical Organic Chemistry, 4th edn., ELBS and Longman, London, 1980, p. 269 and 272.
12 A.I. Vogel, A Text Book of Quantitative Inorganic Analysis, 3rd edn., ELBS and Longman, London, 1980, p. 269, 272, 389, 390 and 480.
13 H.H. Horowitz and G. Metzger, Anal. Chem., 35 (1963) 1464.
14 A.W. Coats and J.P. Redfern, Nature, 201 (1964) 394.
15 E.S. Freeman and B. Carroll, J. Phys. Chem., 62 (1958) 394.
16 H.J. Borchardt and F. Daniels, J. Am. Chem. Soc., 79 (1957) 41.
17 R. Roy, M. Chaudhuri, S.K. Mandal and K. Nag, J. Chem. Soc. Dalton Trans., (1984) 1681.
18 K. Nakamoto, Infrared and Raman Spectra of Inorganic and Co-ordination Compounds, 3rd edn., Wiley Interscience, New York, 1978, p. 226, 322.